ELECTRONIC SUPPLEMENTARY INFORMATION (ESI)

Title:

Determination of ZFS parameters from the EPR spectra of mono-, di- and trinuclear Mn^{II} complexes: impact of magnetic coupling

Authors:

Luis Escriche-Tur, Mercè Font-Bardia, Belén Albela, Montserrat Corbella.

Content:

Table S1. Crystal data and structure refinement details for compounds **1**, **2**, and **3**.

	1	**2**	**3**
Formula	$C_{56}H_{46}Cl_2Mn_2N_8O_{14}$	$C_{56}H_{46}Cl_2Mn_2N_8O_{14}$	$C_{56}H_{46}Cl_2Mn_2N_8O_{14}$
Fw (g/mol)	1235.79	1235.79	1235.79
Crystal colour, habit	Yellow, prism	Yellow, prism	Yellow, prism
***T* (K)**	293(2)	90(2)	293(2)
λ (Mo-Kα) / Å	0.71073	0.71073	0.71073
Crystal size (mm)	0.2 x 0.1x 0.1	0.19x 0.12 x 0.10	0.2 x 0.1 x 0.1
Crystal system	Triclinic	Monoclinic	Triclinic
Space group	*P*-1	*P*21/*c*	*P*-1
***a* / Å**	8.494(4)	9.1362(4)	9.1240(6)
***b* / Å**	13.051(5)	23.6792(10)	12.579(6)
***c* / Å**	14.288(5)	12.2498(5) A	13.411(6)
α / º	113.12(2)	90	63.45(2)
β / º	105.19(3)	92.8570(10)	88.31(4)
γ / º	92.03(3)	90	84.21(4)
***V* / Å³**	1388.6(10)	2646.80(19)	1369.6(9)
Z	1	2	1
ρ_{calcd} / g·cm^{-3}	1.478	1.551	1.498
μ / mm^{-1}	0.625	0.656	0.634
***F*(000)**	634	1268	634
θ range / º	1.625 to 29.966	2.232 to 41.336	1.698 to 32.436
Completeness (to θ / º)	92.6% (25.242)	99.9% (41.336)	93.6%(25.242)
Index ranges	$h = -9 \rightarrow 10$	$h = -16 \rightarrow 16$	$h = -12 \rightarrow 11$
	$k = -17 \rightarrow 16$	$k = -43 \rightarrow 43$	$k = -18 \rightarrow 18$
	$l = -19 \rightarrow 19$	$l = -22 \rightarrow 22$	$l = -18 \rightarrow 20$
Data/restraints/param.	6090 / 15 / 407	17755 / 0 / 370	7910 / 3 / 361
GooF on F^2	1.059	1.085	1.088
R_1[a], ωR_2[b] [$I > 2\sigma(I)$]	0.0344, 0.0971	0.0356, 0.0898	0.0739, 0.1971
R_1[a], ωR_2[b] (all data)	0.0384, 0.1003	0.0471, 0.0952	0.1109, 0.2216

[a] $R_1 = \sum ||F_o| - |F_c|| / \sum |F_o|$. [b] $\omega R_2 = \{\sum[\omega(F_o^2 - F_c^2)^2] / \sum[\omega(F_o^2)^2]\}^{1/2}$, $\omega = 1 / [\sigma^2(F_o^2) + (aP)^2 + bP]$, where $P = [\max(F_o^2, 0) + 2F_c^2] / 3$.

Table S2. Crystal data and structure refinement details for compounds **5**, **6**, and **7**.

	5	**6**	**7**
Formula	$C_{70}H_{58}Cl_2Mn_2N_8O_{12}$	$C_{64}H_{46}Cl_2Mn_2N_8O_{14}$	$C_{64}H_{46}Cl_2Mn_2N_8O_{14}$
Fw (g/mol)	1384.02	1331.87	1331.87
Crystal colour, habit	Yellow, prism	Yellow, prism	Yellow, plaque
***T* (K)**	302(2)	100(2)	100(2)
λ (Mo-Kα) / Å	0.71073	0.71073	0.71073
Crystal size (mm)	0.21 x 0.18 x 0.17	0.32 x 0.30x 0.26	0.28 x 0.13 x 0.05
Crystal system	Triclinic	Triclinic	Monoclinic
Space group	*P*-1	*P*-1	*C*2/*m*
***a* / Å**	10.516(4)	9.5795(16)	9.1362(4)
***b* / Å**	12.247(4)	12.309(2)	23.6792(10)
***c* / Å**	13.821(5)	13.644(3)	12.2498(5)
α / º	67.567(13)	64.358(7)	90
β / º	84.331(17)	84.369(7)	92.8570(10)
γ / º	78.406(16)	84.183(7)	90
***V* / Å³**	1611.3(10)	1440.3(5)	2646.80(19)
Z	1	1	2
ρ_{calcd} / g·cm^{-3}	1.426	1.536	1.592
μ / mm^{-1}	0.545	0.609	0.632
***F*(000)**	714	682	1364
θ range / º	2.489 to 28.775	2.141 to 32.213	2.650 to 30.583
Completeness (to θ / º)	94.0% (25.242)	99.6% (32.213)	99.7% (30.583)
Index ranges	$h = -13 \rightarrow 13$	$h = -14 \rightarrow 14$	$h = -20 \rightarrow 21$
	$k = -15 \rightarrow 15$	$k = -18 \rightarrow 18$	$k = -28 \rightarrow 28$
	$l = -17 \rightarrow 17$	$l = -20 \rightarrow 20$	$l = -13 \rightarrow 11$
Data/restraints/param.	6619 / 4 / 427	10146 / 0 / 424	4379 / 8 / 239
GooF on F^2	1.020	1.061	1.173
R_1[a], ωR_2[b] [$I > 2\sigma(I)$]	0.0659, 0.1290	0.0476, 0.1143	0.0736, 0.1680
R_1[a], ωR_2[b] (all data)	0.2201, 0.2160	0.0644, 0.1221	0.0801, 0.1714

[a] $R_1 = \sum ||F_o| - |F_c|| / \sum |F_o|$. [b] $\omega R_2 = \{\sum[\omega(F_o^2 - F_c^2)^2] / \sum[\omega(F_o^2)^2]\}^{1/2}$, $\omega = 1 / [\sigma^2(F_o^2) + (aP)^2 + bP]$, where $P = [\max(F_o^2, 0) + 2F_c^2] / 3$.

Table S3. Crystal data and structure refinement details for compounds **8**, **9**, and **12**.

	8	**9**	**12**
Formula	$C_{32}H_{25}ClMnN_4O_8$	$C_{28}H_{26}MnN_2O_8$	$C_{72}H_{64}Mn_3N_6O_{18}$
Fw (g/mol)	683.95	573.45	1466.11
Crystal colour, habit	Yellow, prism	Yellow, prism	Yellow, prism
***T* (K)**	100(2)	293(2)	293 (2)
λ (Mo-Kα) / Å	0.71073	0.71073	0.71073
Crystal size (mm)	0.12 x 0.11 x 0.09	0.58 x 0.22 x 0.15	0.1 x 0.09 x 0.07
Crystal system	Triclinic	Monoclinic	Triclinic
Space group	*P*-1	*Cc*	*P*-1
***a* / Å**	8.2965(7)	25.088(3)	11.201(10)
***b* / Å**	13.4504(10)	20.956(3)	11.519(7)
***c* / Å**	14.3581(12)	20.011(3)	14.455(10)
α / º	102.403(3)	90	71.58(4)
β / º	91.449(4)	102.342(5)	71.09(4)
γ / º	106.589(3)	90	74.74(5)
***V* / Å^3**	1493.3(2)	10278(2)	1647(2)
Z	2	16	1
ρ_{calcd} / g·cm^{-3}	1.521	1.482	1.478
μ / mm^{-1}	0.592	0.569	0.645
***F*(000)**	702	4752	757
θ range / º	2.422 to 27.975	2.288 to 28.341	1.539 to 32.411
Completeness (to θ / º)	95.2% (25.242)	99.6% (28.341)	93.3% (25.000)
Index ranges	h = -10 → 10	h = -32 → 33	h = -15 → 16
	k = -17 → 17	k = -27 → 27	k = -17 → 17
	l = -18 → 18	l = -26 → 26	l = -21 → 21
Data/restraints/param.	6591 / 136 / 451	24219 / 4 / 1406	9765 / 0 / 448
GooF on F^2	1.141	1.070	1.050
R_1[a], ωR_2[b] [$I > 2\sigma(I)$]	0.0607, 0.1143	0.0407, 0.0871	0.0859, 0.1881
R_1[a], ωR_2[b] (all data)	0.0821, 0.1238	0.0528, 0.0944	0.1628, 0.2190

[a] $R_1 = \sum ||F_o| - |F_c|| / \sum |F_o|$. [b] $\omega R_2 = \{\sum[\omega(F_o^2 - F_c^2)^2] / \sum[\omega(F_o^2)^2]\}^{1/2}$, $\omega = 1 / [\sigma^2(F_o^2) + (aP)^2 + bP]$, where $P = [\max(F_o^2, 0) + 2F_c^2] / 3$.

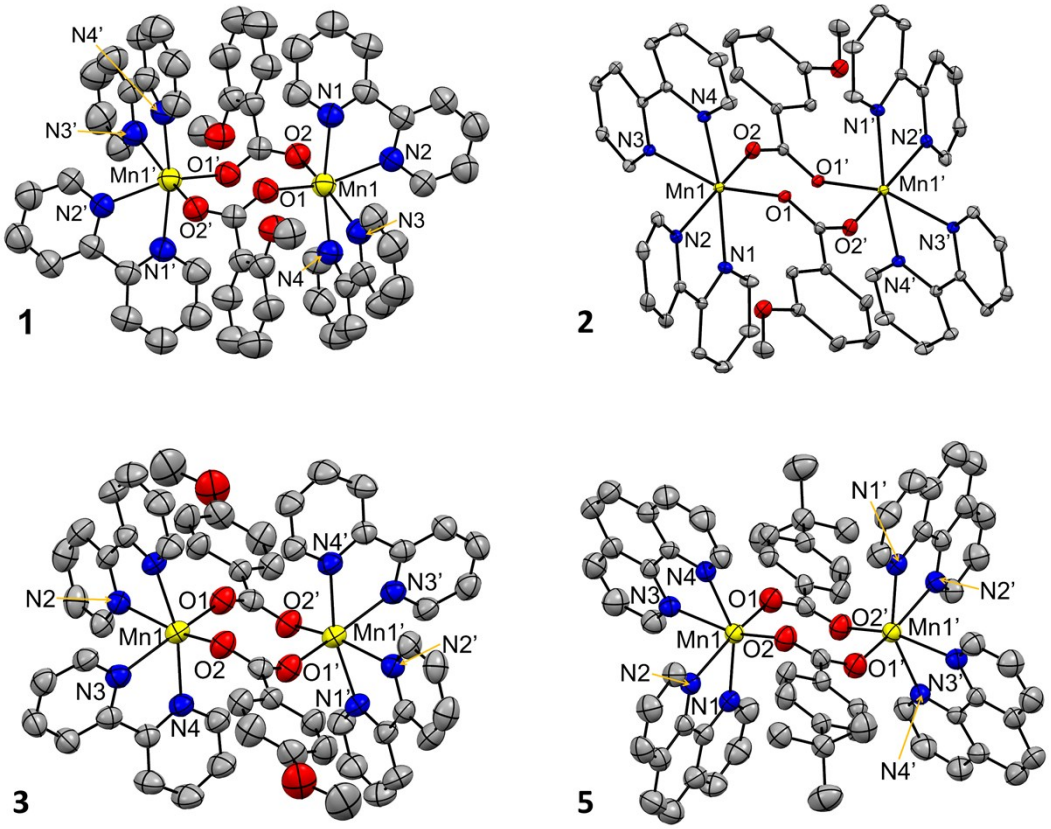

Figure S1. Crystal structures of the cationic complexes of compounds **1**, **2**, **3**, and **5**, showing the anisotropic displacements as ellipsoids at 50% probability. Hydrogen atoms are omitted for clarity.

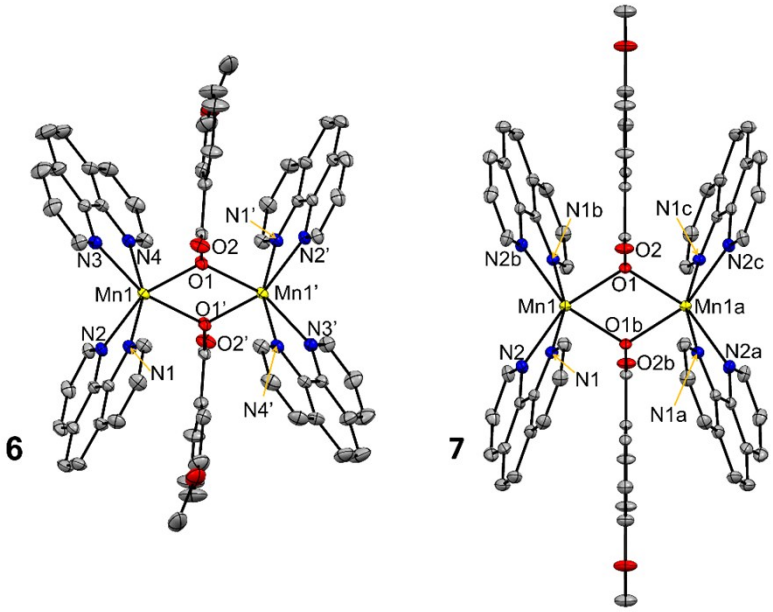

Figure S2. Crystal structures of the cationic complexes of compounds **6** and **7**, showing the anisotropic displacements as ellipsoids at 50% probability. Hydrogen atoms are omitted for clarity.

Table S4. Selected interatomic distances (Å) and angles (deg) with standard deviations in parentheses for compounds **1**, **2**, **3**, and **5**.

	1 (2-MeO, bpy)		**2 (3-MeO, bpy)**
Mn1···Mn1'	4.751(2)	Mn1···Mn1'	4.6396(7)
Mn1–O1	2.1072(17)	Mn1–O1	2.1341(6)
Mn1–O2	2.1242(16)	Mn1–O2	2.1093(7)
Mn1–N1	2.2778(19)	Mn1–N1	2.2506(7)
Mn1–N2	2.2771(18)	Mn1–N2	2.2855(7)
Mn1–N3	2.2732(19)	Mn1–N3	2.3070(8)
Mn1–N4	2.2749(19)	Mn1–N4	2.2375(7)
O2–Mn1–N3	162.55(6)	O1–Mn1–N3	159.77(2)
O1–Mn1–N2	157.13(6)	O2–Mn1–N2	169.74(3)
N4–Mn1–N1	168.75(6)	N4–Mn1–N1	165.99(3)
	3 (4-MeO, bpy)		**5 (4-^{t}Bu, phen)**
Mn1···Mn1'	4.542(2)	Mn1···Mn1'	4.604(2)
Mn1–O1	2.130(3)	Mn1–O1	2.091(3)
Mn1–O2	2.127(3)	Mn1–O2'	2.140(4)
Mn1–N1	2.258(3)	Mn1–N1	2.292(3)
Mn1–N2	2.296(3)	Mn1–N2	2.295(3)
Mn1–N3	2.299(4)	Mn1–N3	2.359(5)
Mn1–N4	2.261(3)	Mn1–N4	2.287(3)
O1–Mn1–N3	161.42(11)	O1–Mn1–N2	164.63(13)
O2–Mn1–N2	162.60(11)	O2'–Mn1–N3	159.86(11)
N1–Mn1–N4	165.77(14)	N1–Mn1–N4	155.09(13)

Symmetry codes: for **1**, (’): 1-x,-y,-z; for **2**, (’) 1-x,2-y,-z; for **3**, (’) 1-x,-y,1-z, for **5**; (’) 1-x;1-y,2-z.

Table S5. Selected interatomic distances (Å) and angles (deg) with standard deviations in parentheses for compounds **6** and **7**.

	6 (3-MeO, phen)		**7 (4-MeO, phen)**
Mn1···Mn1'	3.4596(7)	Mn1···Mn1a	3.4442
Mn1–O1	2.1616(15)	Mn1–O1	2.1825(18)
Mn1–O1'	2.1930(14)	Mn1–O1b	2.1825(18)
Mn1–N1	2.2606(16)	Mn1–N1	2.260(3)
Mn1–N2	2.2546(18)	Mn1–N2	2.267(3)
Mn1–N3	2.2592(16)	Mn1–N1b	2.260(3)
Mn1–N4	2.2579(16)	Mn1–N2b	2.267(3)
O1–Mn1–N2	157.74(5)	N1b–Mn1–N1	161.08(9)
O1'–Mn1–N3	161.61(6)	O1–Mn1–N2	159.26(9)
N4–Mn1–N1	158.61(6)	O1b–Mn1–N2b	159.26(9)
Mn1–O1–Mn1'	105.21(5)	Mn1–O1b–Mn1a	104.19(12)

Symmetry codes: for **6**, (’): -x+1,-y,-z+1; for **7**, (a) x,-y,z, (b) -x,y,-z

Table S6. Selected interatomic distances (Å) and angles (deg) with standard deviations in parentheses for the mononuclear compound **8** and for one of the subunits of compound **9**.

	8 (3-MeO, phen)		**9 (2-MeO, phen)**
Mn1–O1	2.134(2)	Mn1–O1	2.154(4)
Mn1–O4	2.173(3)	Mn1–O3	2.156(4)
Mn1–N1	2.257(3)	Mn1–O5	2.164(3)
Mn1–N2	2.270(3)	Mn1–O6	2.179(3)
Mn1–N3	2.271(3)	Mn1–N2	2.266(4)
Mn1–N4	2.263(3)	Mn1–N1	2.285(4)
N1–Mn1–N4	161.70(10)	O1–Mn1–O3	174.77(13)
O1–Mn1–N2	163.31(9)	O6–Mn1–N1	172.81(14)
O4–Mn1–N3	160.02(9)	O5–Mn1–N2	166.01(13)

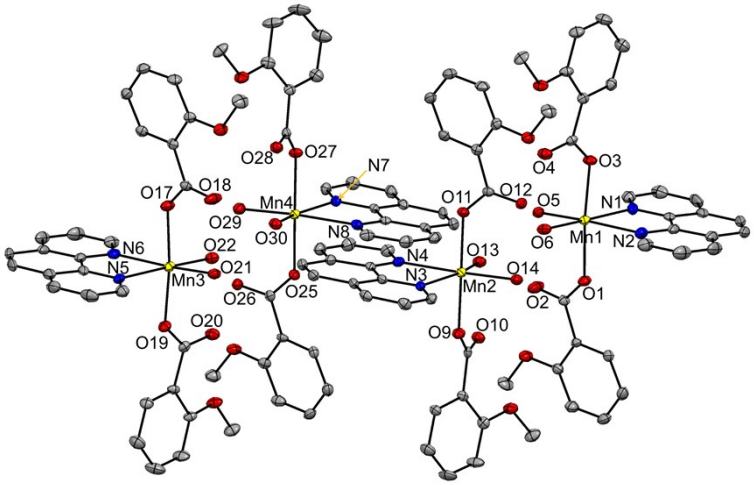

Figure S3. Crystal structure for compound **9**, showing the anisotropic displacements as ellipsoids at 50% probability. Hydrogen atoms are omitted for clarity.

Table S7. Selected interatomic distances (Å) and angles (deg) with standard deviations in parentheses for the mononuclear compound **9**.

Mn1–O1	2.154(4)	Mn3–O19	2.149(4)
Mn1–O3	2.156(4)	Mn3–O21	2.161(3)
Mn1–O5	2.164(3)	Mn3–O17	2.163(4)
Mn1–O6	2.179(3)	Mn3–O22	2.182(3)
Mn1–N2	2.266(4)	Mn3–N6	2.268(4)
Mn1–N1	2.285(4)	Mn3–N5	2.291(4)
O1–Mn1–O3	174.77(13)	O19–Mn3–O17	173.71(12)
O6–Mn1–N1	172.81(14)	O21–Mn3–N6	166.46(13)
O5–Mn1–N2	166.01(13)	O22–Mn3–N5	172.24(13)
Mn2–O9	2.150(4)	Mn4–O27	2.152(4)
Mn2–O11	2.159(4)	Mn4–O25	2.165(3)
Mn2–O13	2.183(3)	Mn4–O30	2.175(3)
Mn2–O14	2.183(3)	Mn4–O29	2.184(3)
Mn2–N3	2.293(4)	Mn4–N7	2.284(4)
Mn2–N4	2.303(3)	Mn4–N8	2.311(3)
O9–Mn2–O11	176.49(10)	O27–Mn4–O25	175.40(13)
O13–Mn2–N3	158.76(12)	O30–Mn4–N7	158.68(12)
O14–Mn2–N4	169.95(13)	O29–Mn4–N8	170.22(13)

Table S8. Selected interatomic distances (Å) and angles (deg) with standard deviations in parentheses for compound **12**.

Mn1···Mn2	3.595	O1–Mn1–N2	160.68(14)
Mn1···Mn1a	7.190(5)	O3–Mn1–N1	162.58(15)
Mn1–O1	2.253(4)	O5–Mn1–O2	160.30(15)
Mn1–O2	2.327(3)	O6a–Mn2–O6	180.00
Mn1–O3	2.102(4)	O4–Mn2–O4a	180.00
Mn1–O5	2.095(4)	O1–Mn2–O1a	180.00
Mn1–N1	2.294(4)		
Mn1–N2	2.256(4)	Mn2–O1–Mn1	105.90(12)
Mn2–O1	2.251(4)		
Mn2–O4	2.200(4)		
Mn2–O6	2.145(4)		

Symmetry codes: (a) -x+1,-y+1,-z

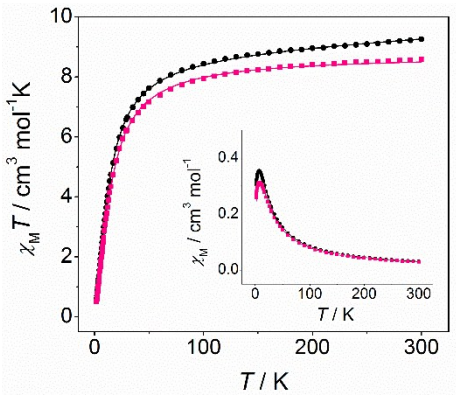

Figure S4. $\chi_M T$ versus T plots and χ_M versus T (inset) for compounds **4** (black circles) and **5** (pink squares).

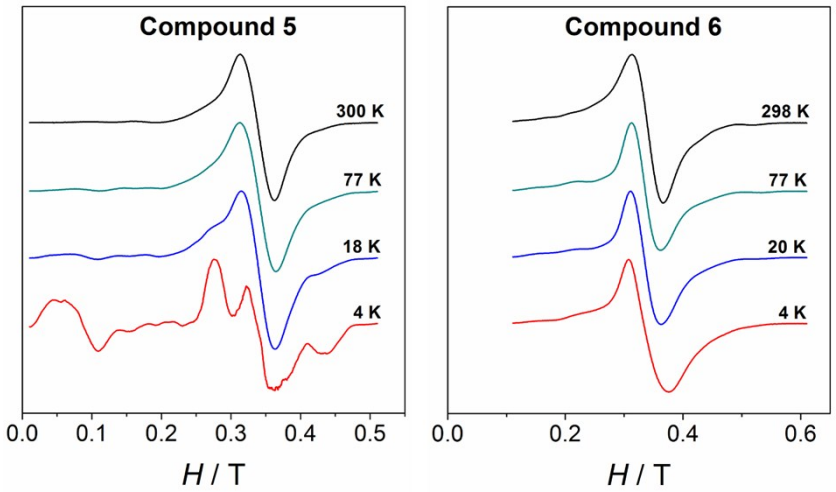

Figure S5. Variable-temperature X-band EPR spectra for the antiferromangetic dinuclear compound **5** and the ferromagnetic dinuclear compound **6**.

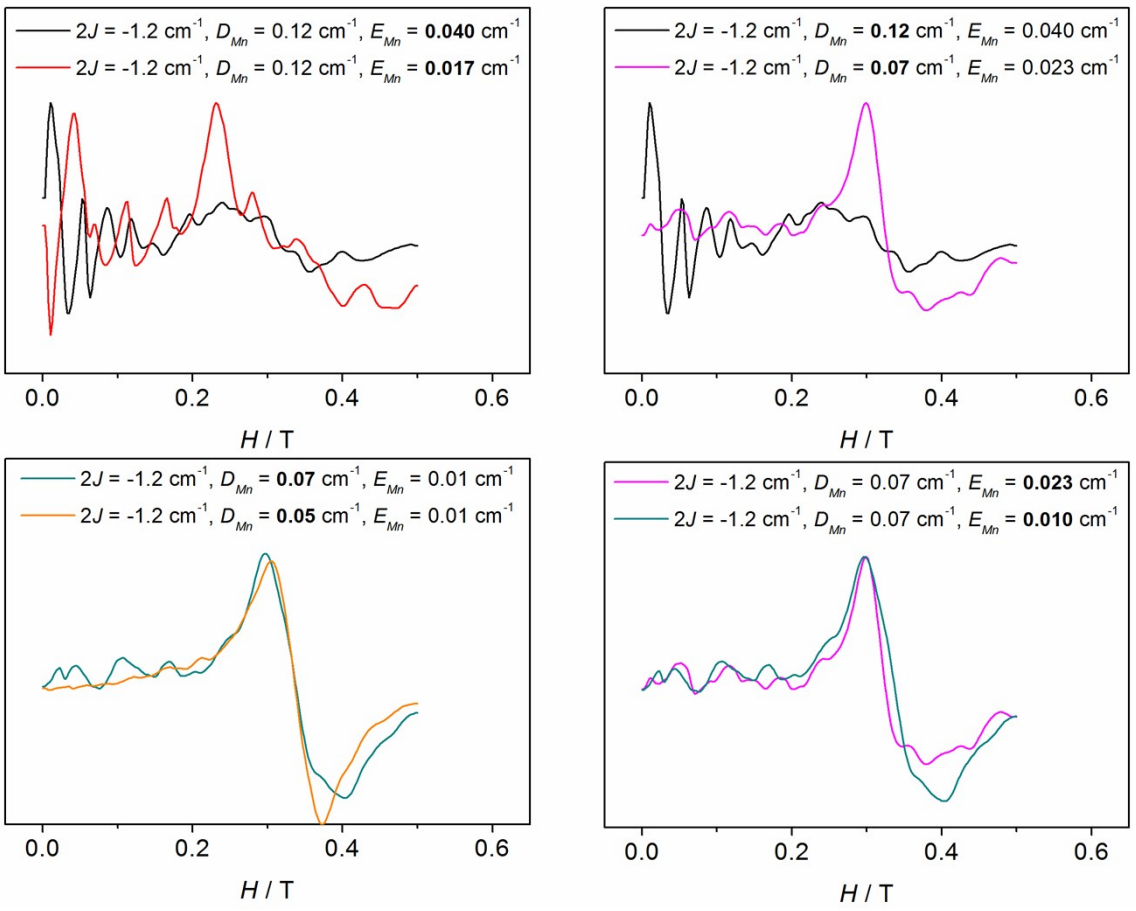

Figure S6. Simulated X-band EPR spectra at 4 K for ferromagnetic dinuclear systems with different D_{Mn} and E_{Mn} values.

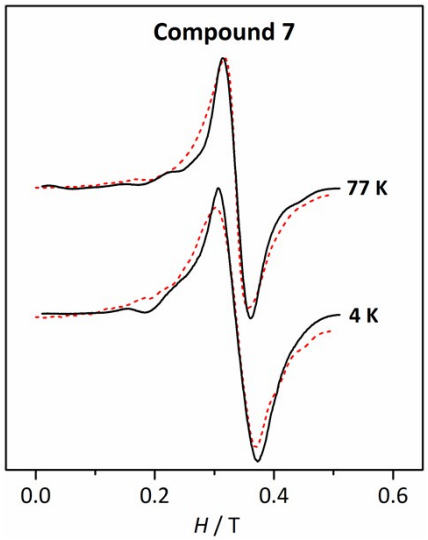

Figure S7. X-band EPR spectra for the ferromagnetic dinuclear compound **7** at 4 and 77 K. The dashed lines correspond to the simulations performed with $2J = -1.3$ cm^{-1}, $|D_{Mn}| = 0.05$ cm^{-1} and $|E_{Mn}| = 0.009$ cm^{-1}.

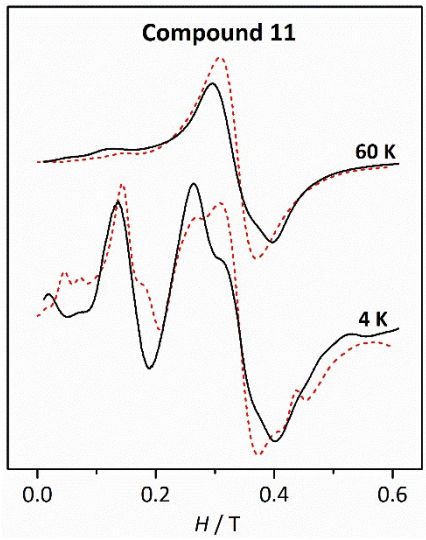

Figure S8. X-band EPR spectra for the trinuclear compound **11** at 4 and 60 K. The dashed lines correspond to the simulations performed with $2J = -2.1$ cm^{-1}, $|D_{Mn}| = 0.09$ cm^{-1} and $|E_{Mn}| = 0.025$ cm^{-1}.

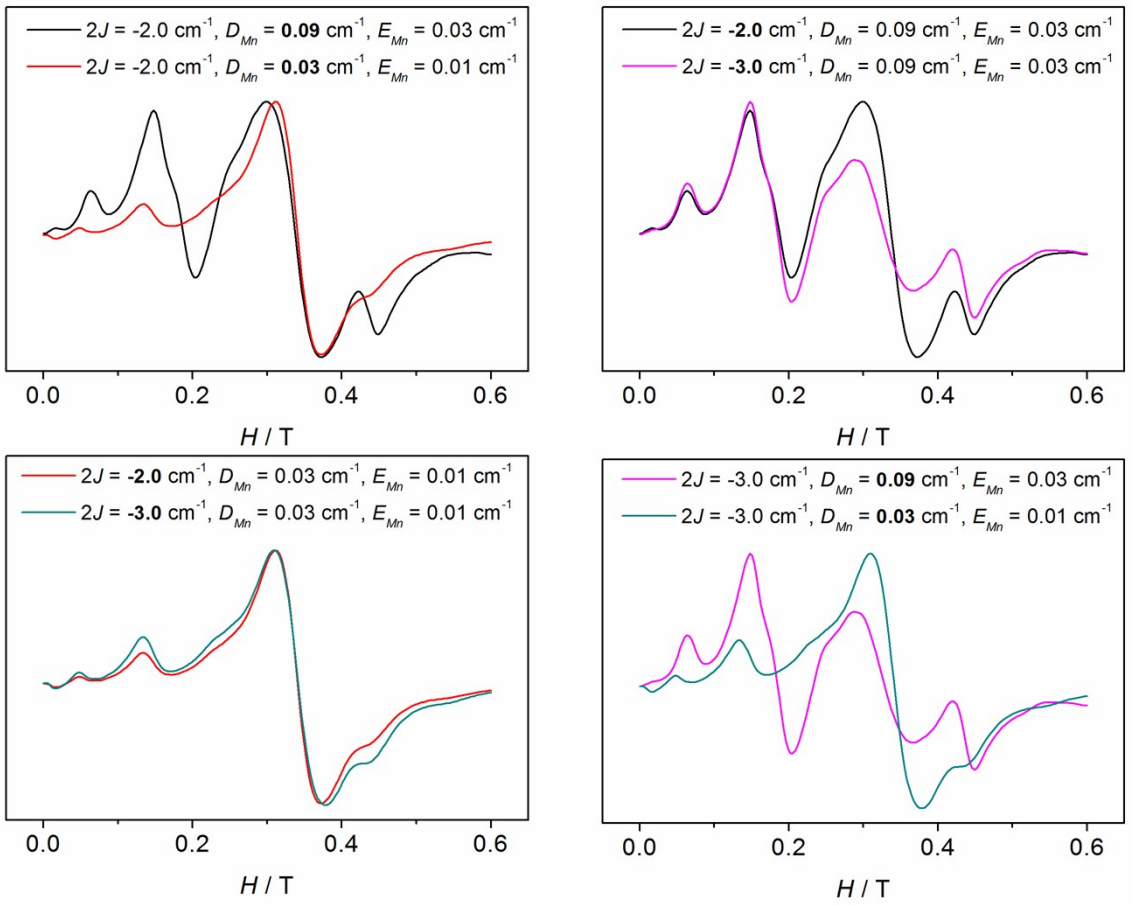

Figure S9. Simulated X-band EPR spectra at 4 K for trinuclear systems with different $2J$, D_{Mn} and E_{Mn} values.

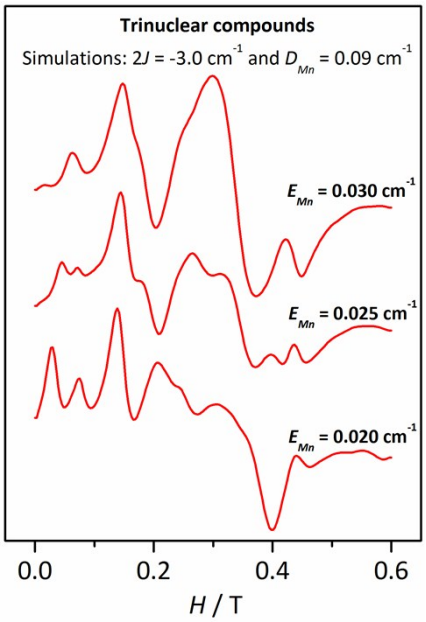

Figure S10. Simulated X-band EPR spectra at 4 K for a trinuclear system with $2J = -3.0$ cm^{-1}, $|D_{Mn}| = 0.09$ cm^{-1}, and $|E_{Mn}| = 0.020$, 0.025, and 0.030 cm^{-1}.